https://doi.org/10.51459/futajeet.2021.15.2.218

Journal of Engineering and Engineering Technology

PERFORMANCE EVALUATION OF RAILWAY BALLAST DEGRADATION USING THE MORPHOLOGICAL PROPERTIES

[1]* Mohammed, A. [1]Aliyu I. [1]Umar H. A, [1] Mani, A. U
[1]Department of Civil Engineering, Ahmadu Bello University, Zaria

ARTICLE HISTORY
Received: 03-04-20
Accepted: 07-12-20

KEYWORDS:
Ballast, degradation, Los Angeles Abrasion, Morphology

ABSTRACT

Ballast degradation through attrition and breakage during operations affects the structural performance of the railway track system and hence in this study, an attempt was made to study railway ballast degradation due to cyclic loading at a micro-scale through quantifying and comparing the changes that occur on ballast particles due to ballast degradation using Los Angeles Abrasion (LAA) test and image analysis techniques. The TB/T 2328.14-2008 gradation used by china railways was adopted and a series of LAA tests test drum in a sequence of 250 turns were conducted to accelerate the ballast particle breakage and abrasion, the changes in the gradation were quantified while the morphological properties were quantified using Aggregate Image Measurement System (AIMS)). At the end of the study, the overall results showed that ballast degradation has a strong correlation with the changes in ballast particle's morphological properties. The relationships and the indices of morphological changes can be used for numerical modeling and simulations through which the discrete element method (DEM) can be used to study the performance of ballast at different degradation levels.

Correspondence: *ibshazali03@hotmai.com*

1.0 INTRODUCTION

Ballasted track system is the most commonly used for the railway transportation system globally. Every year, a large amount of money is being invested in constructing new lines as a result of the fast-growing demand for massive freight movement. Ballast is an essential component of the substructure of a ballasted railway track system whose deterioration leads to failure of the track system. According to (Saussine *et al.,* 2014), Ballast is a uniformly-graded coarse aggregate, which consists of crushed hard rocks with particle sizes ranges from 12.5 mm to 63 mm, placed under and between the sleepers, with high density, toughness, hardness, and high resistance to weathering. Ballast is primarily provided to give support for the sleepers, transfer stresses from the bearing area of the sleepers to the surface of the subgrade soil or sub-ballast, and to provide rapid drainage for the ballasted rail track. (Lu and McDowell, 2010). Ballast aggregates undergo abrasion and degradation under repeated traffic loading, the sliding action between aggregate particles results in degradation of aggregates through attrition

https://doi.org/10.51459/futajeet.2021.15.2.218

and produce pulverized ballast particle, which contributes to the fouling of ballast voids (Ionescu, 2004). Fouling refers to the infiltration of fines (fines from the ballast aggregate breakdown, coal dust from coal trains, subgrade soil intrusion, and sleepers wearing) into the voids of the unbound granular layer of the railroad ballast. (Qian *et al.,* 2017). Salig and waters, (1994) Stated that ballast particles degradation contributes largely to the fouling of the rail ballast layer approximately by 76%, and 24% is due to the infiltration of fines from the surface of the ballast, intrusion of subgrade materials, and the wearing of the sleepers. To assess ballast field performance associated with degradation caused by the particle to particle attrition of angular asperities and breakage, a considerable amount of experimental studies have been carried out by numerous researchers to generate fouled ballast materials from ballast degradation processes in the laboratory using standard empirical tests, such as; the Los Angeles (LA) abrasion test, crushing value (ACV), micro-Deval abrasion test, Deval abrasion test, and mill abrasion test (Qian *et al.,* 2017). Lim, (2004) and McDowell *et al.,* (2005) Researched by simulating the effects of both train loading and ballast tamping provided on four granitic rocks and revealed that there was a correlation between the Los Angeles Abrasion (LAA) test and ballast degradation(Nålsund et al., 2013; Qian et al., 2014; Qian *et al.,* 2017). Aursudkij, (2007) conducted similar research on three different types of rock. He concluded that Los Angeles Abrasion (LAA) test results correlate well with ballast degradation. In 2013, Nålsund *et al.,* (2013) performed a comparative assessment of ballast degradation using large-scale triaxial and full-scale rail track model tests with mechanical laboratory tests on Norwegian ballast materials. The results revealed that the LA abrasion test results correlated with the actual material breakdown better than micro-Deval abrasion test results. Qian *et al.* (2014 and 2017) conducted an experimental study to characterise ballast aggregate degradation using LA abrasion tests and aggregate image analysis. The results revealed that LA abrasion tests could generate fouled ballast through accelerating ballast degradation with abrasion. And a good correlation between the ballast fouling index and the morphological properties of the aggregate indices was observed.

However, in an attempt to know the in-depth effect of ballast degradation on railway ballast bed performance, this study quantified the ballast particle morphological changes in relation to the particle degradations. Ballast particle morphology includes the particle shape, texture, and particle size(Guo et al., 2020), it is considered to be a crucial factor that affects macro-micro mechanical behaviour and physical properties of granular materials(Nie et al., 2020); the packing, bulk density, contacts (coordination number), particle degradation and porosity(Dahal et al., 2018). Because of this, a series of LAA tests need to be performed to quantify the changes in the ballast particles' morphological properties (i.e., flakiness and elongation, surface texture, and angularity) and also to ascertain the ballast degradation on the specimen.

2.1 Material

The ballast material used for this study was a

100% crushed granite collected from Xiangxiang quarry about 114km away from Changsha in Hunan province, china. The aggregates with different particle sizes were carefully selected, washed, oven-dried, and air-dried at room temperature and then sieved separately. The specimens were remixed together according to the target proportion, as per the People's Republic of China Railway Industry-standard gradation (TB/T 2328.14-2008) requirements as shown in Figure 1.

2.2 Methods

The Los Angeles abrasion (LAA) test coupled with Imaging technics were employed for this research and were conducted in accordance with the standard specifications.

2.2.1 Los Angeles Abrasion test

The Los Angeles abrasion (LAA) test procedure was following ASTM Standard C535 (ASTM, 2009), which involved placing 10 kg of fresh ballast material with 12 steel balls into the LAA drum. The drum was set to rotate at an average of 33 revolutions per minute, and for each run, the drum rotated 250 times. Afterward, the drum was allowed to stand still for 10-15 min to let the dust settle before the evacuation of the tested material. The inner part of the drum and the steel balls were carefully hand brushed to collect dust and fine material. The tested materials were sieved and cleaned thoroughly to collect dust and fine material using a sieve shaker to minimise loss of fines. Material passing each sieve was collected and recorded. Particles larger than 9.5mm (3/8-in) were collected for image analysis using the Aggregate Image Measurement System (AIMS).

2.2.2 Imaging of ballast Aggregates

Aggregate Image Measurement System (AIMS) was developed to quantify aggregate shape characteristics using computer-controlled motion, image processing, and analysis techniques. The aggregate measurement is characterized in terms of its shape, angularity, and surface texture (Gates *et al.,* 2011). Figure 2. Shows an illustration of the AIMS system. The image analysis technique has been in use for over two decades and has provided an in-depth knowledge of the morphological behaviour of aggregate particles (Qian *et al.,* 2017). The AIMS software was used to determine the essential morphological indices (are the angularity index (AI), the surface texture (ST) index, and the flatness and elongated (F&E) ratio). These three key indices are as illustrated in Figure 3. AIMS angularity index quantifies the total changes in the particle edge sharpness characteristics on a scale of 0-10000. It is categorized into four groups (low, moderate, high, and extremely angular), as illustrated in Figure 4. The F&E ratio quantifies the ratio of the longest to the shortest dimensions of a particle in an assembly of flat, elongated, cubical particles. The Surface Texture (ST) index quantifies the roughness of a particle through an erosion-dilation image analysis technique on a scale of 0-1000. It is also categorized into four groups, as illustrated in Figure 5. The image analysis was conducted to ascertaining the changes in particle size and shape after each test before mixing all materials for the next LA abrasion run. The procedure was repeated at an interval of 250 turns of LA abrasion drum until the number of turns reached 2000.

https://doi.org/10.51459/futajeet.2021.15.2.218

Marsal's breakage ratio (B_g) was used in this study to quantify the amount of ballast degradation. The breakage ratio proposed by Marsal, (1967) is determined as the summation of positive values of the difference in percentage by mass of total material retained on the same sieve size after the test (Koohmishi and Palassi, 2018). The differences in percentage retained on each sieve size (ΔW_k) is determined as follows;

$$\Delta W_k is W_{ki} - W_{kf} \quad (1)$$

Where W_{ki} and W_{kf} ; are the percentages by mass retained on sieve size k before and after the test respectively. Marsal's breakage ratio (B_g) was adopted for this study because of its simplicity and accuracy (Indraratna and Salim, 2002).

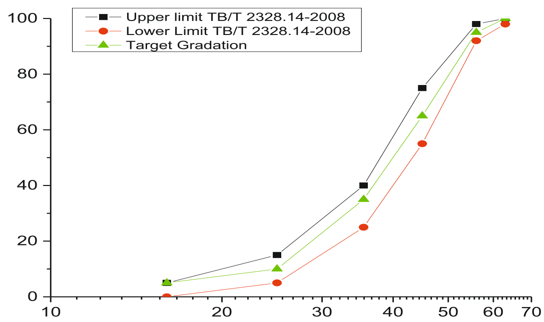

Figure 1 Gradation of crushed granite ballast material (TB/T 2328.14-2008, 2008)

Figure 2. Second-generation of AIMS

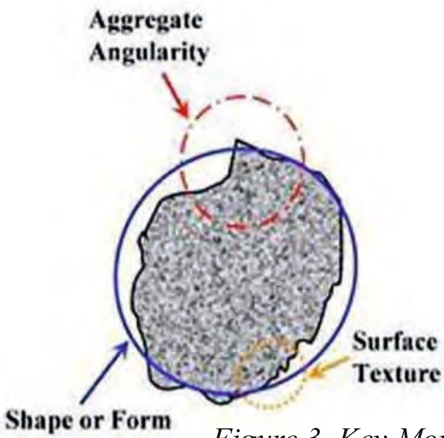

Figure 3. Key Morphological descriptors ***(Masad and Fletcher, 2005)***

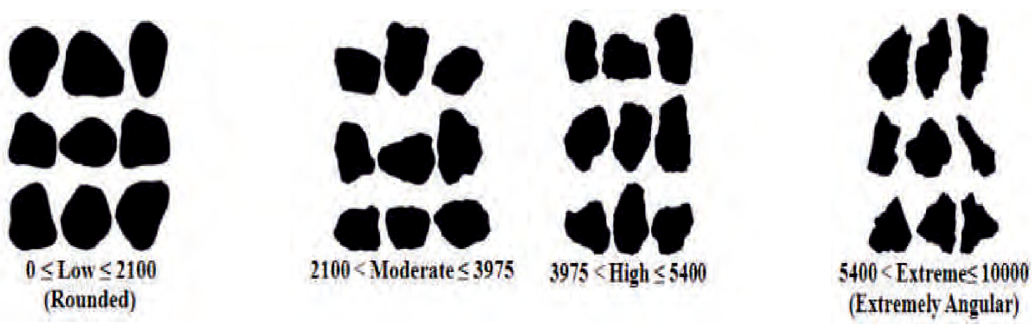

Figure 4. Particles Angularity categories indicating scale index (March 2010)

https://doi.org/10.51459/futajeet.2021.15.2.218

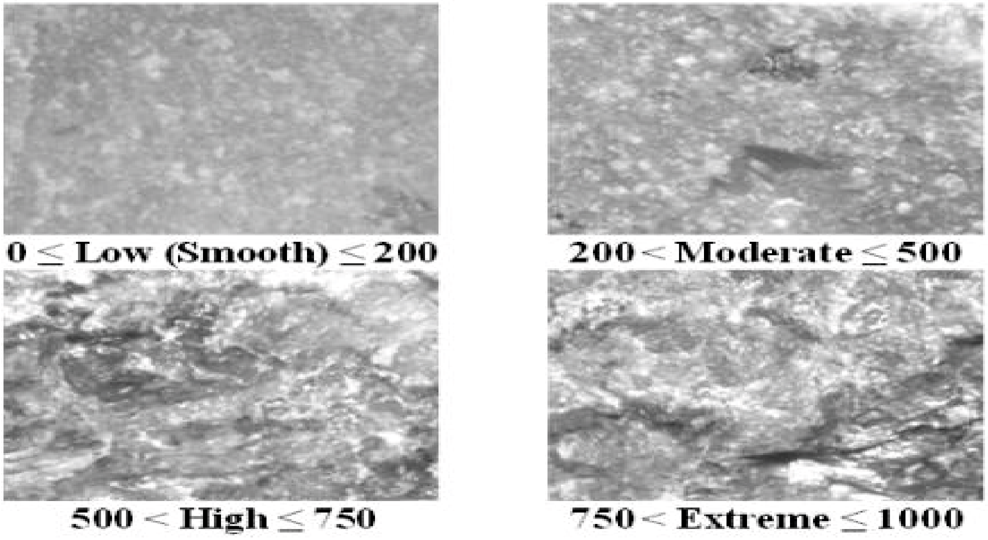

Figure 5. Classifications of Particles Surface Texture according to scale index (March 2010

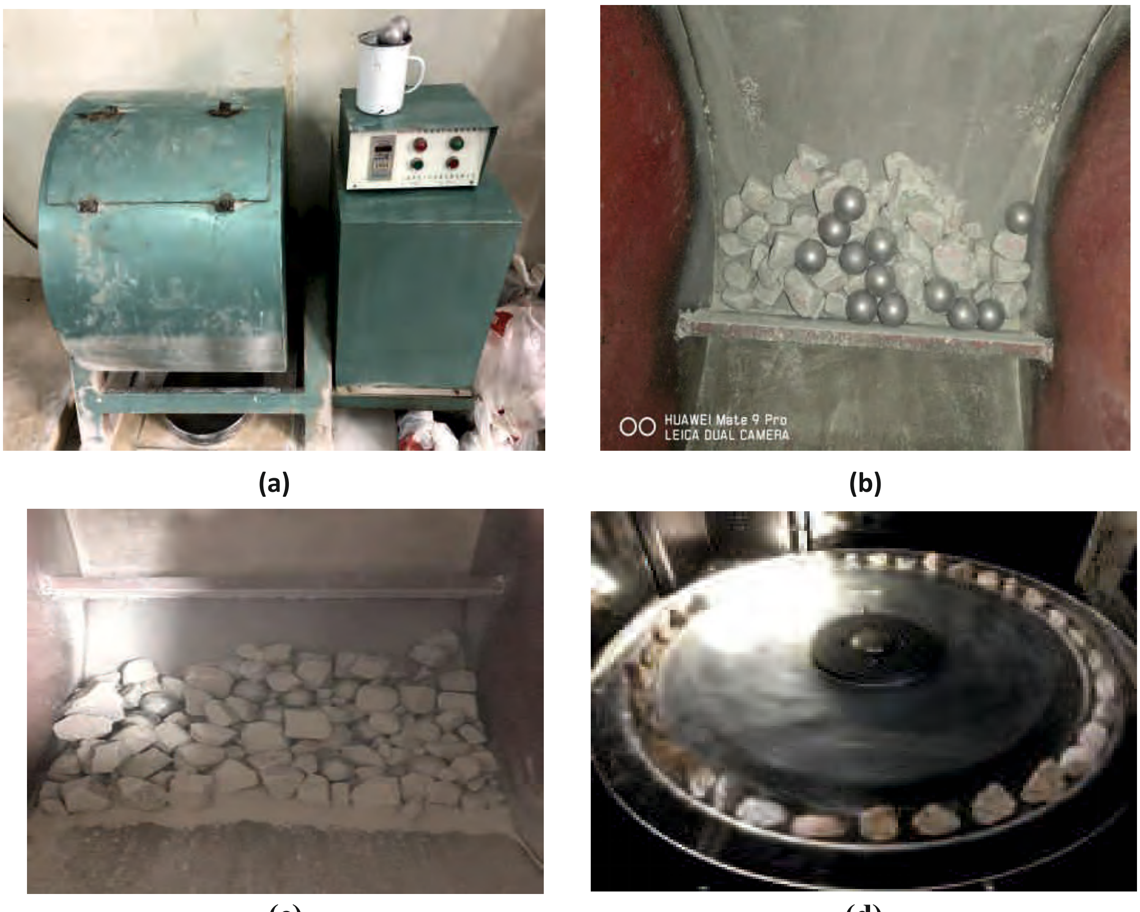

(a) **(b)**

(c) **(d)**

Figure 6. LA abrasion test machine and AIMS tray with specimen: (a) LA abrasion test device, (b) ballast and steel balls before test, (c) ballast and steel balls after test, and (d) Specimen on AIMS tray

https://doi.org/10.51459/futajeet.2021.15.2.218

3.0 Results and Discussion

3.1 Gradation

The results for the LA abrasion test are as presented in Figure 7. The Figure shows the gradation curves obtained from the sieve analysis of the ballast after 2000 turns of the LA abrasion drum at an interval of 250 turns. The Figure also presents the corresponding values of the breakage ratio obtained after every 250 turns of the LAA test drum. It can be seen that with an increase in the number of turns of the LA abrasion drum, the specimen's gradations shift gradually to the left making the specimen denser and reducing the void ration of the samples.

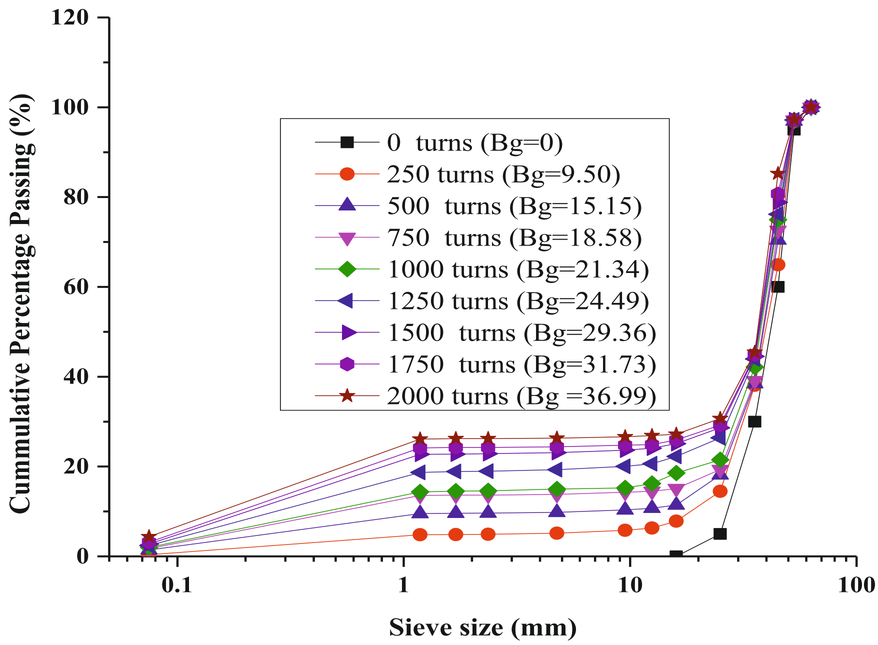

Figure 7 Gradation changes of ballast specimen after LAA test

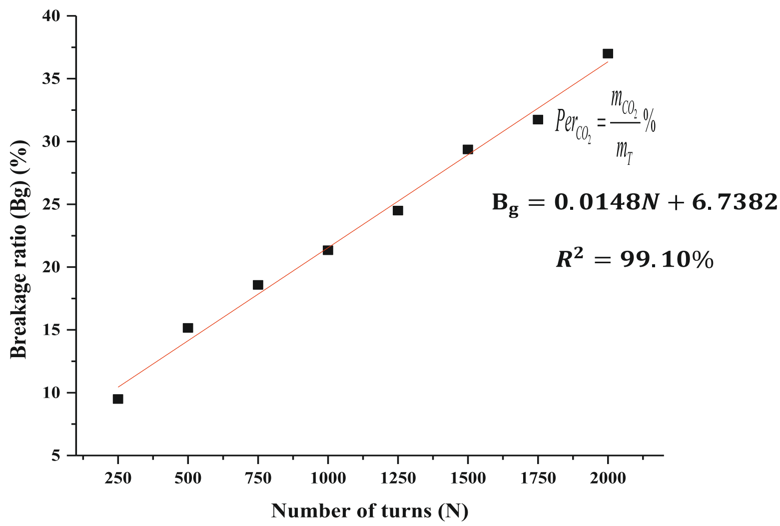

Figure 8 Breakage index values Against Number LA abrasion tests.

https://doi.org/10.51459/futajeet.2021.15.2.218

Figure 8 presents the ballast degradation trends in-terms of Marsal's breakage ratio (B_g) values. It is clearly shown that with an increase in the number of LAA drum turns, the breakage ratio (B_g) values increases. The increase in breakage ratio can be attributed to the breakage and splitting of larger particles into smaller particles and becomes rounded due to the abrading of the particles' sharp edges with an increase in the number of LAA drum turns, this consequently decreases the ballast shear strength, particle to particle interlock, and drainage capacity and increases axial deformation of the ballast layer. Therefore, ballast degradation in the field is attributed primarily to the breakage of sharp corners during service; this agrees with the works of (Indraratna *et al.,* 2014, Indraratna *et al.,* 2013, Qian *et al.,* 2017).

3.2 Morphological Properties

The changes in morphological features of ballast aggregate during the degradation process were investigated using the AIMS (aggregate image measurement system) package in the laboratory. Figure 9 illustrates the changes in the shape and texture of a single aggregate particle inform of images at intervals of the number of LA abrasion drum turns. The morphological indices computed by the imaging analysis software are; AI angularity index, ST Surface texture, and F&E flat and elongated ratio. It can be seen that with an increase in the number of LA abrasion drum turns, the particle becomes rounded and smoother, and hence all the image-based indices decrease. For example, at 0 turns of LA abrasion drum, the ballast particle was rough, angular, and has sharp edges, its' imaging-based shape indices were respectively 2,643.220, 393.870, and 1.517 for AI, ST, and F&E while at 2000 turns the indices were 1,675.32, 250.984, and 1.198 respectively.

Table 1 presents the average values of shape indices obtained against the number of LAA test drum turns. A decrease in average angularity index and surface texture index with an increase in LAA test drum turns can be observed from the table, The average AI for all particle sizes at 0, 1000, and 2000 LAA test drum turns are respectively 2980, 2140, and 1795. Similarly, the average ST for all particle sizes at 0, 1000, and 2000 LAA test drum turns are respectively 302, 221, and 217, while the flatness and elongation index follows no definite trend. However, at some smaller particle sizes and LAA test drum turns, the slight increase of the index could be due to the larger particle breakage and split into smaller particles forming a new rough surface. This trend is an explicit confirmation that the individual particles tend to be rounded and smoother with an increase in the number of LA abrasion drum turns, except in a situation where a particle breaks up and forms a new rough surface. The results further confirmed that large particles are more prone to breakage during service.

Figure 10 shows the correlation between the percentage changes in average angularity index (AI) with breakage index (B_g) values. The polynomial trend line was found to be the perfect relationship for the data. a coefficient of determination $R^2$of 98.93% was computed between the angularity changes and breakage index.

Similarly, Figure 11 also shows a strong correlation between percentage changes in

https://doi.org/10.51459/futajeet.2021.15.2.218

Angularity	Texture	Shape Index
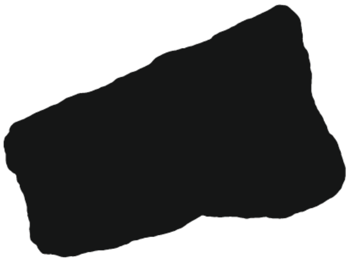	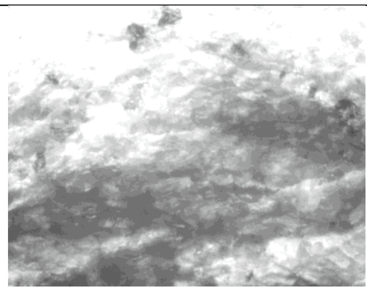	**At 0 turns** **AI: 2643.22** **F&E:1.517** **ST: 293.870**
	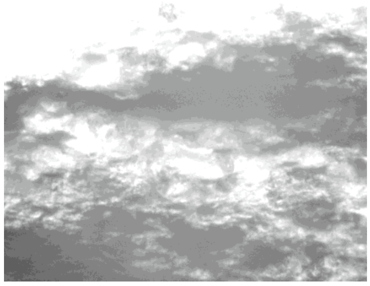	**After 500 turns** **AI: 2383.67** **F&E:1.508** **ST: 221.880**
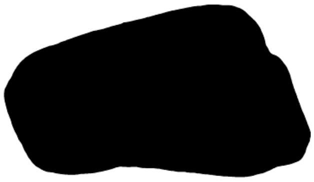	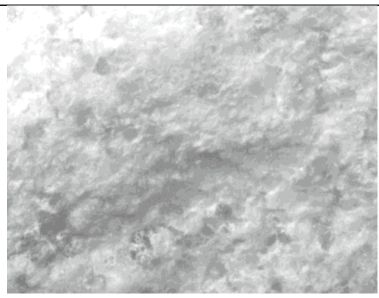	**After1000 turns** **AI: 2283.18** **F&E:1.444** **ST: 204.810**
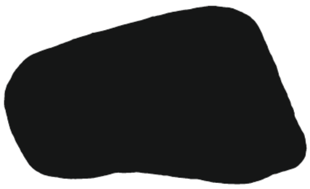	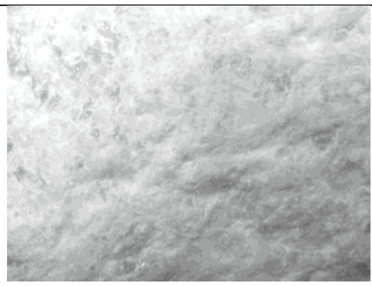	**After1500 turns** **AI: 1980.13** **F&E: 1.314** **ST: 168.051**
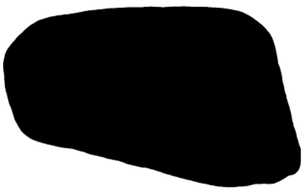	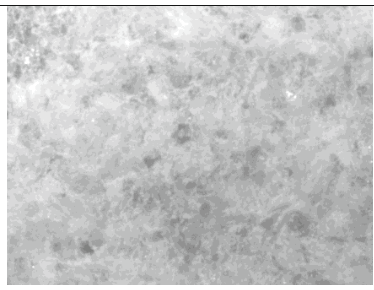	**After 2000 turns** **AI: 1675.32** **F&E: 1.198** **ST: 150.984**

Figure 9; AIMS based images of shape and texture properties of a single particle throughout the degradation process based on LA abrasion testing

https://doi.org/10.51459/futajeet.2021.15.2.218

Table 1. Image-Based Shape indices

Shape Index	Sieve Size (mm)	NUMBER OF TURNS								
		0	250	500	750	1000	1250	1500	1750	2000
Angularity Index	53	-	-	-	-	-	-	-	-	-
	45	2980	2339	2272	2261	2140	2133	2126	2090	1795
	35.5	2762	2281	2047	1944	1892	1735	1733	1694	1761
	25	2823	2215	2064	2000	1921	1812	1765	1749	1718
	16	2882	2318	2089	2081	2074	2057	1948	1794	1852
	12.5	2345	2119	2168	2000	2233	2227	2208	2107	2208
	9.5	-	2312	2443	2358	2327	2380	2288	2550	2423
	AVERAGE	**2758**	**2264**	**2180**	**2107**	**2098**	**2057**	**2011**	**1997**	**1959**
Surface Texture Index	53	-	-	-	-	-	-	-	-	-
	45	278	280	205	200	188	203	209	196	195
	35.5	285	252	238	232	228	179	209	205	198
	25	340	262	232	226	202	212	199	203	201
	16	304	236	234	226	242	222	230	230	220
	12.5	302	258	233	229	248	236	246	249	266
	9.5	-	252	218	224	219	273	231	229	220
	AVERAGE	**302**	**257**	**226**	**223**	**221**	**221**	**221**	**218**	**217**
Flatness and Elongation	53	-	-	-	-	-	-	-	-	-
	45	1.44	1.47	1.47	1.58	1.44	1.41	1.41	1.60	1.46
	35.5	1.58	1.59	1.52	1.65	1.53	1.56	1.48	1.52	1.47
	25	1.57	1.61	1.74	1.64	1.62	1.71	1.67	1.64	1.62
	16	2.60	1.74	1.80	1.89	1.80	1.82	1.79	1.79	1.69
	12.5	2.54	2.32	2.01	2.04	1.89	1.72	1.58	1.65	1.81
	9.5	-	2.02	1.89	1.81	1.91	1.91	1.75	1.67	1.37
	AVERAGE	**1.95**	**1.79**	**1.74**	**1.77**	**1.70**	**1.69**	**1.61**	**1.65**	**1.57**

average surface texture index (ST) with breakage index (B_g) values with a coefficient of determination R^2 of 91.56%. The trends presented in Figures 10 and 11 show a reasonable linkage between the breakage index (B_g) with the overall changes in shape (angularity and surface texture) indices of ballast material. These relationships agree with the findings of Qian *et al.*, (2017) and Moaveni *et al.,* (2013). The relationships and the indices of the morphological changes can be used for numerical modeling and simulations using discrete element modelling (DEM) to study the performance of ballast at different degradation levels.

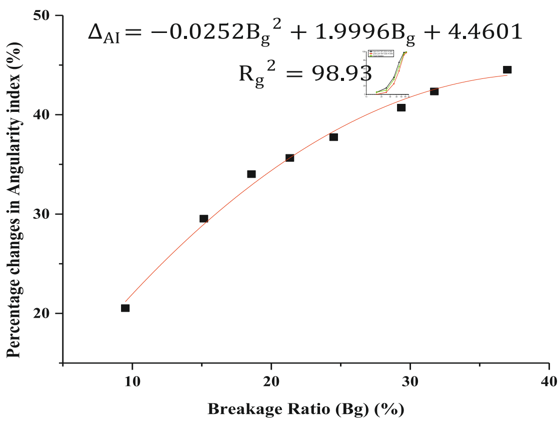

Figure 10. Percentage changes in the Angularity index related to the breakage index.

https://doi.org/10.51459/futajeet.2021.15.2.218

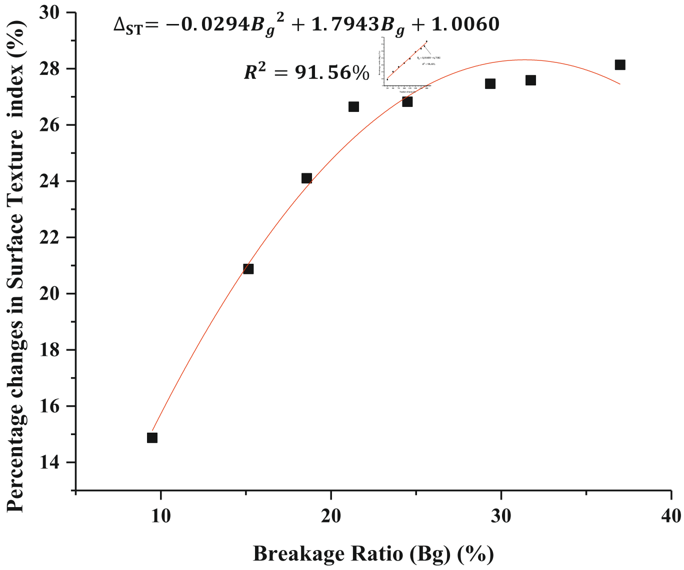

Figure 11. Percentage changes in surface texture index related to the Breakage index

CONCLUSION

This paper presents an experimental study on railway ballast degradation and its morphological changes. The ballast particle gradations and morphological properties were analysed during the degradation process at an interval of 250 turns of the LA abrasion test drum, from the fresh ballast to degraded ballast at 2000 revolution of the LA abrasion test drum. Image-based assessment of particles larger than 9.5mm revealed the changes in the particle morphological properties (angularity index, surface texture index, and flatness and elongation ratio) during the degradation. The breakage ratio (B_g) values increase with an increase in the number of LA abrasion drum turns, which is due to the chipping off of sharp edges, abrading of surface, and break down of larger particles into smaller sizes. At the end of the study, the overall results showed that ballast degradation has a strong correlation with the changes in ballast particle's morphological properties. The relationships and the indices of morphological changes can be used for numerical modeling and simulations through which the discrete element method (DEM) can be used to study the performance of ballast at different degradation levels.

REFERENCE

ASTM, A. (2009) C535-09 Standard Test Method for Resistance to Degradation of Large Size Coarse Aggregate by Abrasion and Impact in the Los Angeles Machine. Conshohocken, PA: ASTM.

Aursudkij, B. (2007) *A laboratory study of railway ballast behaviour under traffic loading and tamping maintenance*. University of Nottingham.

China. TMOR. Test method for ballast of railway gravel road (TB/T 2328.6-2008): Railway Industry Standard of the People's Republic of China, 2008.

Dahal, B., Mahmud, S. & Mishra, D.

https://doi.org/10.51459/futajeet.2021.15.2.218

(2018), Simulating Ballast Breakage Under Repeated Loading Using the Discrete Element Method. 2018 Joint Rail Conference, American Society of Mechanical Engineers Digital Collection.

Gates, L., Masad, E., Pyle, R. and Bushee, D. (2011), Aggregate Image Measurement System 2 (AIMS2): Final Report. FHWA-HIF-11-030, Highways for LIFE Program Office, Pine Instrument Company.

Guo, Y., Zhao, C., Markine, V., Jing, G. and Zhai, W. (2020) Calibration for discrete element modelling of railway ballast: A review. *Transportation Geotechnics*, 100341.

Indraratna, B. and Salim, W. (2002) Modelling of particle breakage of coarse aggregates incorporating strength and dilatancy.

Indraratna, B., Nimbalkar, S., Coop, M. and Sloan, S. W. (2014) A constitutive model for coal-fouled ballast capturing the effects of particle degradation. *Computers and Geotechnics,* 61**,** 96-107.

Indraratna, B., Tennakoon, N. C., Nimbalkar, S. S. and Rujikiatkamjorn, C. (2013) Behaviour of clay-fouled ballast under drained triaxial testing.

Ionescu, D. (2004) Ballast Degradation and Measurement of Ballast Fouling, 7th Railway Engineering Proceedings, 5-6 July. *London, UK*, 169-180.

Koohmishi, M. and Palassi, M. (2018) Degradation of railway ballast under compressive loads considering particles rearrangement. *International Journal of Pavement Engineering*, 1-13.

Lim, W. L. 2004. *Mechanics of railway ballast behaviour.* University of Nottingham.

Lu, M. and Mcdowell, G. (2010) Discrete element modelling of railway ballast under monotonic and cyclic triaxial loading. *Géotechnique,* 60**,** 459.

March (2010) Aggregate Image Measurement System: Model AFA2A Operation Manual. *Pine Instrument Company, Grove City, Pa.*

Marsal, R. J. (1967) Large-scale testing of rock-fill materials. *Journal of the Soil Mechanics and Foundations Division,* 93**,** 27-43.

Masad, E. and Fletcher, T. (2005). Aggregate imaging system (AIMS): Basics and applications. Texas Transportation Institute, Texas A & M University System.

Mcdowell, G. R., Lim, W. L., Collop, A. C., Armitage, R. and Thom, N. H. (2005) Laboratory simulation of train loading and tamping on ballast. Proceedings of the institution of civil engineers-transport, 2005. Thomas Telford Ltd, 89-95.

Moaveni, M., Wang, S., Hart, J. M., Tutumluer, E. and Ahuja, N. (2013) Evaluation of aggregate size and shape by means of segmentation techniques and aggregate image processing algorithms. *Transportation Research Record,* 2335**,** 50-59.

Nålsund, R., Tutumuler, E. and Horvli, I. (2013), Degradation of railway ballast through large scale triaxial and full-scale rail track model tests. Proceedings of the international conferences on the bearing capacity of roads, railways and airfields, 2013. 807-819.

Nie, Z., Fang, C., Gong, J. and Liang, Z. (2020) DEM study on the effect of

https://doi.org/10.51459/futajeet.2021.15.2.218

roundness on the shear behaviour of granular materials. *Computers and Geotechnics,* 121**,** 103457.

Qian, Y., Boler, H., Moaveni, M., Tutumluer, E., Hashash, Y. M. and Ghaboussi, J. (2014) Characterizing ballast degradation through Los Angeles abrasion test and image analysis. *Transportation Research Record,* 2448**,** 142-151.

Qian, Y., Boler, H., Moaveni, M., Tutumluer, E., Hashash, Y. M. and Ghaboussi, J. (2017) Degradation-related changes in ballast gradation and aggregate particle morphology. *Journal of Geotechnical and Geoenvironmental Engineering,* 143**,** 04017032.

Saussine, G., Quezada, J., Breul, P. and Radjai, F. (2014), Railway Ballast Settlement: A New Predictive Model. Proceedings of the Second International Conference on Railway Technology: Research, Development and Maintenance", Civil-Comp Press, Stirlingshire, UK, Paper,

Selig, E. T., and Waters, J. M. (1994). Track geotechnology and substructure management. *Thomas Telford, Ltd., London.*